DESY 00–169
UG–FT–125/00
hep-ph/0012305
December 2000

Top flavour-changing neutral coupling signals at a linear collider

J. A. Aguilar–Saavedra
Departamento de Física Teórica y del Cosmos
Universidad de Granada
E-18071 Granada, Spain

Abstract

We present an analysis of the sensitivity of the TESLA e^+e^- collider to top flavour-changing neutral couplings to the Z boson and photon. We consider the cases without beam polarization, with only e^- polarization and with e^- and e^+ polarization, showing that the use of the latter substantially enhances the sensitivity to discover or bound these vertices. For some of the couplings the expected LHC limits could be improved up to an order of magnitude for equal running times.

1 Introduction

It is widely believed that the top quark, because of its large mass, will be a sensitive probe into physics beyond the Standard Model (SM) [1]. In particular, its couplings to the gauge and Higgs bosons may show deviations with respect to the SM predictions. We will focus on flavour-changing neutral (FCN) interactions involving the top, a light charge 2/3 quark q and a neutral gauge boson $V = Z, \gamma$. In the SM the FCN couplings Vtq vanish at tree-level but can be generated at the one-loop level. However, they are very suppressed by the GIM mechanism, because the masses of the charge $-1/3$ quarks in the loop are small compared to the scale involved. The calculation of the branching ratios for top decays mediated by these FCN operators yields the SM predictions $\mathrm{Br}(t \to Zc) = 1.3 \times 10^{-13}$, $\mathrm{Br}(t \to \gamma c) = 4.5 \times 10^{-13}$ [2], and smaller values for the up quark. However, in many simple SM extensions these rates can be orders of magnitude larger. For instance, in models with exotic quarks $\mathrm{Br}(t \to Zq)$ can be of order 10^{-3} [3]. Two Higgs doublet models allow for $\mathrm{Br}(t \to Zc) = 10^{-6}$, $\mathrm{Br}(t \to \gamma c) = 10^{-7}$ [4], and in R parity-violating supersymmetric models one can have $\mathrm{Br}(t \to Zc) = 10^{-4}$, $\mathrm{Br}(t \to \gamma c) = 10^{-5}$ [5]. Top FCN decays into a light Higgs boson and an up or charm quark can also have similar or larger rates in these models [6, 4, 7]. Hence, top FCN couplings offer a good place to search for new physics, which may manifest if these vertices are observed in future colliders. At present the best limits on Ztq couplings come from LEP 2, $\mathrm{Br}(t \to Zq) \leq 0.07$ [8, 9], and the best limits on γtq couplings from Tevatron, $\mathrm{Br}(t \to \gamma q) \leq 0.032$ [10]. They are very weak but will improve in the next years, first with Tevatron Run II, and later with the next generation of colliders.

The CERN LHC will be a top factory. With a $t\bar{t}$ production cross-section of 830 pb, at its 100 fb^{-1} luminosity phase it will produce 8.3×10^7 top-antitop pairs per year, and 3×10^7 single tops plus antitops via other processes [11, 12]. This makes LHC an excellent machine for the investigation of the top quark properties. The search for FCN top couplings can be carried out examining two different types of processes. On the one hand, we can look for rare top decays $t \to Zq$ [13], $t \to \gamma q$ [14], $t \to gq$ [15] or $t \to Hq$ [16] of the tops or antitops produced in the SM process $gg, q\bar{q} \to t\bar{t}$. On the other hand, one can search for single top production via an anomalous effective vertex: Zt and γt production [17], the production of

a single top quark [18], and Ht production [16]. In these cases the top quark is assumed to decay in the SM dominant mode $t \to Wb$.

The TESLA e^+e^- collider with a centre of mass (CM) energy $\sqrt{s} = 500$ GeV has a tree-level $t\bar{t}$ production cross-section of 0.52 pb, and produces only 1.56×10^5 top-antitop pairs per year with an integrated luminosity of 300 fb^{-1}. However, e^+e^- colliders are cleaner than hadron colliders. For instance, the signal to background ratio S/B for rare top decays can be 7 times larger in TESLA than in LHC. But the sensitivity to rare top decays is given in the Gaussian statistics limit by the ratio $S/\sqrt{B}$, and the larger LHC cross-sections make difficult for TESLA to compete with it in the search for anomalous top couplings.

Here we show that for single top production [19] the use of beam polarization in TESLA substantially enhances the sensitivity to discover or bound top anomalous FCN couplings and is equivalent to an increase in the luminosity by a factor of $6 - 7$. This allows TESLA to improve some of the expected LHC limits up to an order of magnitude. We consider the planned CM energies of 500 and 800 GeV, and for both we analyse three cases: without beam polarization, with 80% e^- polarization, and with 80% e^-, 45% e^+ polarization. We also study rare top decays in the processes $e^+e^- \to t\bar{t}$, with subsequent decay $\bar{t} \to V\bar{q}$ (or $t \to Vq$). Single top production and top decay processes are complementary: although single top production is more sensitive to top anomalous couplings, top decays can help to disentangle the type of anomalous coupling involved (Ztq or γtq) if a positive signal is discovered.

2 Single top production

In order to describe the FCN couplings among the top, a light quark q and a Z boson or a photon A we use the Lagrangian

$$\begin{aligned} -\mathcal{L} &= \frac{g_W}{2c_W} X_{tq}\, \bar{t}\gamma_\mu (x_{tq}^L P_L + x_{tq}^R P_R) q Z^\mu + \frac{g_W}{2c_W}\, \kappa_{tq}\, \bar{t}(\kappa_{tq}^v - \kappa_{tq}^a \gamma_5) \frac{i\sigma_{\mu\nu} q^\nu}{m_t} q Z^\mu \\ &\quad + e\, \lambda_{tq}\, \bar{t}(\lambda_{tq}^v - \lambda_{tq}^a \gamma_5) \frac{i\sigma_{\mu\nu} q^\nu}{m_t} q A^\mu \,, \end{aligned} \tag{1}$$

where $P_{R,L} = (1 \pm \gamma_5)/2$. The chirality-dependent parts are normalized to $(x_{tq}^L)^2 + (x_{tq}^R)^2 = 1$, $(\kappa_{tq}^v)^2 + (\kappa_{tq}^a)^2 = 1$, $(\lambda_{tq}^v)^2 + (\lambda_{tq}^a)^2 = 1$. This effective Lagrangian contains γ_μ terms of dimension 4 and $\sigma_{\mu\nu}$ terms of dimension 5. The couplings are constants corresponding to the first terms in the expansion in momenta. The $\sigma_{\mu\nu}$ terms are the only ones allowed by the unbroken gauge symmetry, $\mathrm{S}U(3)_c \times \mathrm{U}(1)_Q$. Due to their extra momentum factor they grow with the energy and make single top production at TESLA the best process to measure them.

For single top production we study the process $e^+e^- \to t\bar{q}$ mediated by Ztq or γtq anomalous couplings as shown in Fig. 1, followed by top decay $t \to W^+b \to l^+\nu b$, with $l = e, \mu$. We will only take one type of anomalous coupling different from zero at the same time, and we evaluate three signals: (i) with Ztq γ_μ couplings, setting $x_{tq}^L = x_{tq}^R$ for definiteness; (ii) with Ztq $\sigma_{\mu\nu}$ couplings, taking $\kappa_{tq}^v = 1$, $\kappa_{tq}^a = 0$; (iii) with γtq couplings, taking $\lambda_{tq}^v = 1$, $\lambda_{tq}^a = 0$. However, if a positive signal is discovered, it may be difficult to distinguish only from this process whether the anomalous coupling involves the Z boson, the photon or both. On the other hand, in principle it could be possible to have a fine-tuned cancellation between Z and γ contributions that led to a suppression of this signal.

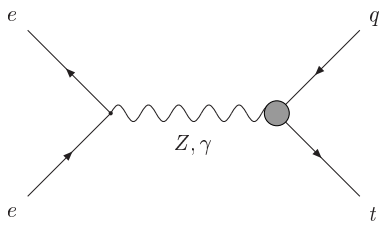

Figure 1: Feynman diagrams for $e^+e^- \to t\bar{q}$ via Ztq or γtq FCN couplings. The top quark is off-shell and has the SM decay.

We calculate the matrix element for $e^+e^- \to t\bar{q} \to W^+b\bar{q} \to l^+\nu b\bar{q}$ using HELAS [20] and introducing a new HELAS-like subroutine `IOV2XX` to compute the non-renormalizable $\sigma_{\mu\nu}$ vertices. This new routine has been checked comparing with calculations done by hand. In all cases we sum $t\bar{q} + \bar{t}q$ production but we sometimes refer to the signals as $t\bar{q}$ for simplicity. The signal cross-sections depend slightly on the chirality of the anomalous couplings. For a CM energy of 500 GeV and the three polarization options discussed the cross-sections for γ_μ and $\sigma_{\mu\nu}$ couplings have a maximum variation of 1.2% for other chirality choices.

The background for the $t\bar{q}$ signal is given by $W^+q\bar{q}'$ production with W^+ decay to electrons and muons. The leading contribution to this process is W^+W^- production with W^- hadronic decay, but it is crucial for the correct evaluation of the background after kinematical cuts to take into account the 7 interfering Feynman diagrams for $e^+e^- \to W^+q\bar{q}'$. Taking all the interfering diagrams for $e^+e^- \to l^+\nu q\bar{q}'$ into account does not give an appreciable difference in the cross-section. This background is evaluated using MadGraph [21] and modifying the code to include the W^+ decay.

To simulate the calorimeter energy resolution we perform a Gaussian smearing of the charged lepton (l), photon (γ) and jet (j) energies using a calorimeter resolution [22] of

$$\frac{\Delta E^{l,\gamma}}{E^{l,\gamma}} = \frac{10\%}{\sqrt{E^{l,\gamma}}} \oplus 1\% \,, \qquad \frac{\Delta E^{j}}{E^{j}} = \frac{50\%}{\sqrt{E^{j}}} \oplus 4\% \,, \tag{2}$$

where the energies are in GeV and the two terms are added in quadrature. For simplicity we assume that the energy smearing for muons is the same as for electrons. Note that more optimistic resolutions would improve our results. We then apply detector cuts on transverse momenta, $p_T \geq 10$ GeV, and pseudorapidities, $|\eta| \leq 2.5$ (this corresponds to polar angles $10^\circ \leq \theta \leq 170^\circ$). We reject the events in which the jets and/or leptons are not isolated, requiring that the distances in (η, ϕ) space satisfy $\Delta R \geq 0.4$. We do not require specific trigger conditions, and we assume that the presence of high p_T charged leptons will suffice.

The signal is reconstructed as follows. The neutrino momentum p_ν can be identified with the missing momentum of the event. The longitudinal missing momentum can also be used, and p_ν is reconstructed without any ambiguity. The W^+ momentum is then the sum of the momenta of the charged lepton and the neutrino. For the signal, the invariant mass of the W^+ and one of the jets, $m_t^{\rm rec}$, is consistent with the top mass, and the other jet has an energy E_q around $E_q^0 \equiv (s - m_t^2)/(2\sqrt{s})$. Of the two possible pairings, we choose the one minimizing $(m_t^{\rm rec} - m_t)^2 + (E_q - E_q^0)^2$. The kinematical distributions of $m_t^{\rm rec}$ for the signal and the background at a CM energy of 500 GeV without beam polarization are plotted in Fig. 2. Then we require a b tag on the jet associated to the decay of the top quark to reduce

the background. To ensure a high charm rejection we apply more strict kinematical cuts on this jet, $|\eta_b| \leq 2$ (polar angle $15^\circ \leq \theta_b \leq 165^\circ$) and energy $E_b \geq 45$ GeV. We assume a b tagging efficiency of 60%, and mistagging rates of 5% for charm and 0.5% for lighter quarks [23]. The E_b kinematical distributions are shown in Fig. 3.

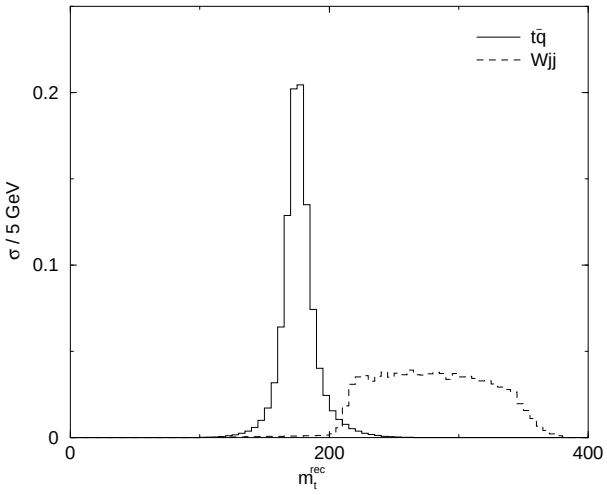

Figure 2: Reconstructed top mass $m_t^{\rm rec}$ distribution before kinematical cuts for the three $t\bar{q}$ signals and W^+jj background at a CM energy of 500 GeV, without beam polarization. The cross-sections are normalized to unity.

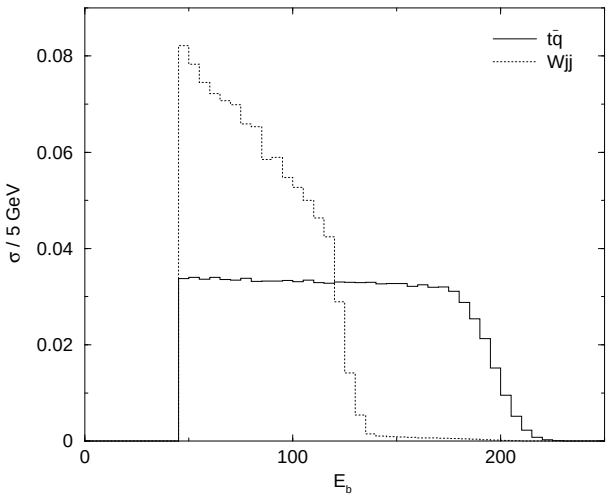

Figure 3: E_b distribution before kinematical cuts for the three $t\bar{q}$ signals and W^+jj background at a CM energy of 500 GeV, without beam polarization. The cross-sections are normalized to unity.

Another interesting variable to distinguish the signal from the background is the two-jet invariant mass $M_{W^-}^{\rm rec}$. The W^+jj background is dominated by W^+W^- production with

$W^- \to jj$, and the $M^{\rm rec}_{W^-}$ distribution peaks around M_W. A veto cut on $M^{\rm rec}_{W^-}$ can eliminate a large fraction of the background but makes compulsory to calculate correctly the cross-section to include all the diagrams for $e^+e^- \to W^+q\bar{q}'$. Also of interest are the total transverse energy H_T and the charged lepton energy E_l in Figs. 4 and 5. The kinematical distributions with polarized beams are very similar except the H_T distribution. In this case polarization decreases the peak of the background around $H_T = 200$.

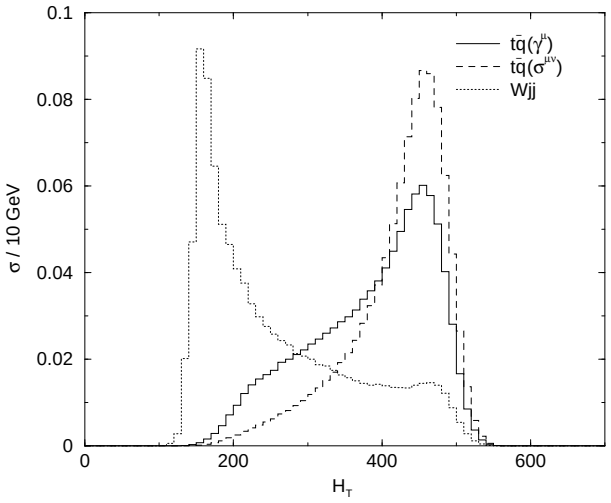

Figure 4: Total transverse energy H_T distribution before kinematical cuts for the three $t\bar{q}$ signals and W^+jj background at a CM energy of 500 GeV, without beam polarization. The cross-sections are normalized to unity.

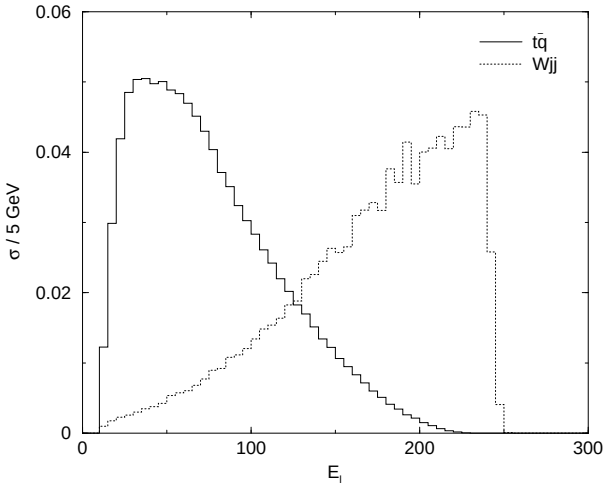

Figure 5: Charged lepton energy E_l distribution before kinematical cuts for the three $t\bar{q}$ signals and W^+jj background at a CM energy of 500 GeV, without beam polarization. The cross-sections are normalized to unity.

To enhance the signal significance we perform kinematical cuts on these variables. However, we find that the veto cut on $M_{W^-}^{\rm rec}$ is unnecessary in single top production since the requirement $E_b > 45$ GeV and the kinematical cut on $m_t^{\rm rec}$ practically eliminate the peak in the $M_{W^-}^{\rm rec}$ distribution. A cut on E_q is unnecessary because this variable is kinematically related to $m_t^{\rm rec}$, and we prefer to apply a cut on $m_t^{\rm rec}$ to show the presence of a top quark in the signal. For simplicity, we choose to apply the same cuts for the three signals and the three polarization options, but different for CM energies of 500 and 800 GeV. We choose the cuts trying to maintain the independence of the cross-section on the chirality of the coupling. Obviously, our results could be improved modifying the cuts for each type of coupling and each polarization option. Before discussing the results it is convenient to outline the procedure used to obtain the limits on the anomalous couplings. The correct statistical treatment of signals and backgrounds is specially necessary in our study since the backgrounds are very small even for high integrated luminosities.

Assuming that no signal is observed after the experiment is done, *i.e.* the number of observed events n_0 equals the expected background n_b, we derive 95% confidence level (CL) upper bounds on the number of events expected n_s. We use the Feldman-Cousins construction for the confidence intervals of a Poisson variable [24] evaluated with the PCI package [25].

On the other hand, we can obtain the smallest value of n_s such that a positive signal is expected to be observed with $3\,\sigma$ significance, assuming that the number of observed events for $3\,\sigma$ 'evidence' n_e equals $n_s + n_b$. For a large number of background events, the Poisson probability distribution can be approximated by a Gaussian of mean n_b and standard deviation $\sqrt{n_b}$. The requirement of $3\,\sigma$ significance is then simply $n_s/\sqrt{n_b} \geq 3$. However, this is seldom the case for our study, where the backgrounds are very small. In such case, we use the estimator based on the $\mathcal{P}$ number (see for example [26]). The number $\mathcal{P}(n)$ is defined as the probability of the background to fluctuate and give n or more observed events. n_e is then defined as the smallest value of n such that $1 - \mathcal{P}(n) \geq 99.73\%$, corresponding to three Gaussian standard deviations.

The limits on the number of signal events obtained in this way can be translated into limits on the anomalous coupling constants, and expressed in terms of top decay branching ratios taking $\Gamma_t = 1.56$ GeV. We now discuss the results for 500 GeV and 800 GeV in turn.

2.1 Limits for $\sqrt{s} = 500$ GeV

The kinematical cuts for 500 GeV are collected in Table 1, and the cross-sections before and after cuts in Table 2. We normalize the signals to $X_{tq} = 0.06$, $\kappa_{tq} = 0.02$, $\lambda_{tq} = 0.02$ and sum $t\bar{q} + \bar{t}q$ production. For different chiralities of the anomalous couplings the cross-sections after cuts differ at most 7% for γ_μ couplings and 5% for $\sigma_{\mu\nu}$ couplings.

Variable	Cut
$m_t^{\rm rec}$	$160 - 190$
H_T	> 220
E_l	< 160

Table 1: Kinematical cuts for the three $t\bar{q}$ signals and the three polarization options at a CM energy of 500 GeV. The masses and the energies are in GeV.

	No pol.		Pol. e^-		Pol. e^- e^+	
	before cuts	after cuts	before cuts	after cuts	before cuts	after cuts
$t\bar{q}+\bar{t}q$ (Z,γ_μ)	0.183	0.137	0.162	0.121	0.215	0.161
$t\bar{q}+\bar{t}q$ $(Z,\sigma_{\mu\nu})$	0.199	0.153	0.176	0.135	0.234	0.179
$t\bar{q}+\bar{t}q$ (γ)	0.375	0.288	0.375	0.287	0.510	0.391
$W^\pm jj$	19.5	0.0734	4.06	0.0154	2.40	0.0092

Table 2: Cross-sections (in fb) before and after the kinematical cuts in Table 1 for the three $t\bar{q}$ signals and their background at a CM energy of 500 GeV, for the three polarization options. We include b tagging efficiencies and use $X_{tq}=0.06$, $\kappa_{tq}=0.02$, $\lambda_{tq}=0.02$.

Polarization is very useful to improve the limits from single top production. In Table 2 we notice that the use of 80% e^- polarization decreases the background by a factor of 5 while keeping 90% of the signal, and additional e^+ polarization of 45% decreases the background by a factor of 8 and increases the signal 20% with respect to the values without polarization. The improvement is clearly seen in the limits of Table 3, obtained for an integrated luminosity of 300 fb^{-1}. e^-, e^+ polarization improves the $3\,\sigma$ discovery limits by factors of $2.8-3.2$. The integrated luminosity required to obtain the same limits without using polarization would be 2100 fb^{-1}.

	No pol.		Pol. e^-		Pol. e^- e^+	
	95%	$3\,\sigma$	95%	$3\,\sigma$	95%	$3\,\sigma$
Br$(t\to Zq)$ (γ_μ)	4.4×10^{-4}	6.1×10^{-4}	3.1×10^{-4}	3.9×10^{-4}	1.9×10^{-4}	2.2×10^{-4}
Br$(t\to Zq)$ $(\sigma_{\mu\nu})$	3.5×10^{-5}	4.8×10^{-5}	2.4×10^{-5}	3.1×10^{-5}	1.5×10^{-5}	1.7×10^{-5}
Br$(t\to\gamma q)$	2.2×10^{-5}	3.0×10^{-5}	1.3×10^{-5}	1.7×10^{-5}	8.2×10^{-6}	9.3×10^{-6}

Table 3: Limits on top FCN decay branching ratios obtained from single top production at 500 GeV with a luminosity of 300 fb^{-1} for the three polarization options.

2.2 Limits for $\sqrt{s}=800$ GeV

We write the kinematical cuts for 800 GeV in Table 4, and the signal cross-sections before and after cuts in Table 5. The cross-sections for $t\bar{q}$ production mediated by non-renormalizable couplings do not decrease raising the CM energy from 500 to 800 GeV, whereas the background decreases to less than one half. This improves the sensitivity for $\sigma_{\mu\nu}$ couplings with respect to 500 GeV. Unfortunately, the signal with γ_μ couplings also decreases, and thus the results are worse in this case.

For equal luminosities, an e^+e^- collider with a CM energy of 800 GeV is sensitive to top rare decays mediated by $\sigma_{\mu\nu}$ vertices with branching ratios $1.5-2$ times smaller than one with 500 GeV. Of course, the higher luminosity at 800 GeV has also to be taken into account, and then this energy is best suited to perform searches for these vertices. Again we observe the usefulness of polarization: the use of e^- polarization reduces the background 5 times and the use of e^+ polarization as well reduces it 8 times. In Table 6 we gather the limits for an integrated luminosity of 500 fb^{-1}. e^-, e^+ polarization improves the $3\,\sigma$ discovery limits by

Variable	Cut
$m_t^{\rm rec}$	$160 - 190$
H_T	> 450
E_l	< 300

Table 4: Kinematical cuts for the three $t\bar{q}$ signals and the three polarization options at a CM energy of 800 GeV. The masses and the energies are in GeV.

	No pol.		Pol. e^-		Pol. e^- e^+	
	before cuts	after cuts	before cuts	after cuts	before cuts	after cuts
$t\bar{q} + \bar{t}q$ (Z, γ_μ)	0.0776	0.0498	0.0684	0.0440	0.0912	0.0586
$t\bar{q} + \bar{t}q$ $(Z, \sigma_{\mu\nu})$	0.198	0.149	0.175	0.132	0.233	0.175
$t\bar{q} + \bar{t}q$ (γ)	0.389	0.293	0.389	0.293	0.528	0.398
$W^{\pm}jj$	8.45	0.0125	1.75	0.0028	1.03	0.0018

Table 5: Cross-sections (in fb) before and after the kinematical cuts in Table 4 for the three $t\bar{q}$ signals and their background at a CM energy of 800 GeV, for the three polarization options. We include b tagging efficiencies and use $X_{tq} = 0.06$, $\kappa_{tq} = 0.02$, $\lambda_{tq} = 0.02$.

factors of $2.5 - 2.9$. The luminosity necessary to obtain the same limits without the use of polarization would be 3000 fb^{-1}.

	No pol.		Pol. e^-		Pol. e^- e^+	
	95%	$3\,\sigma$	95%	$3\,\sigma$	95%	$3\,\sigma$
Br$(t \to Zq)$ (γ_μ)	4.4×10^{-4}	5.9×10^{-4}	2.9×10^{-4}	4.3×10^{-4}	2.4×10^{-4}	2.3×10^{-4}
Br$(t \to Zq)$ $(\sigma_{\mu\nu})$	1.3×10^{-5}	1.7×10^{-5}	8.6×10^{-6}	1.3×10^{-5}	6.2×10^{-6}	7.0×10^{-6}
Br$(t \to \gamma q)$	7.8×10^{-6}	1.0×10^{-5}	4.5×10^{-6}	6.7×10^{-6}	3.7×10^{-6}	3.6×10^{-6}

Table 6: Limits on top FCN decay branching ratios obtained from single top production at 800 GeV with a luminosity of 500 fb^{-1} for the three polarization options.

3 Top decays

For top decays we study the SM process $e^+e^- \to t\bar{t}$, followed by antitop decay mediated by an anomalous Ztq or γtq coupling. This gives the signals $t\bar{q}Z$ and $t\bar{q}\gamma$, and the different final states distinguish Ztq and γtq couplings. The top is assumed to decay via $t \to W^+b \to l^+\nu b$, with $l = e, \mu$. For the $t\bar{q}Z$ signal we only consider the Z boson decays to electrons and muons.

The cross-sections for the $t\bar{q}V$ signals are smaller than for single top production for equal values of the FCN coupling parameters. The reasons are: (i) $t\bar{q}$ production is enhanced by the q^ν factor of the $\sigma_{\mu\nu}$ vertex, when present, whereas $t\bar{q}V$ is not; (ii) the final state cross-section for $t\bar{q}Z$ includes the partial width Br$(Z \to l'^+l'^-) = 0.067$; (iii) phase space for the production of a $t\bar{t}$ pair is smaller than for $t\bar{q}$. However, top decay signals are cleaner than single top production. This can be understood since the top decay signals W^+bjV have

the enhancement over their background W^+jjV of two on-shell particles, the top and the antitop, whereas single top production has only the enhancement due to the top on-shell and the $\sigma_{\mu\nu}$ coupling if that is the case.

For $t\bar{q}Z$ and $t\bar{q}\gamma$ production we calculate the matrix elements $e^+e^- \to t\bar{t} \to W^+b\bar{q}Z \to l^+\nu b\bar{q}l'^+l'^-$ and $e^+e^- \to t\bar{t} \to W^+b\bar{q}\gamma \to l^+\nu b\bar{q}\gamma$, respectively, using HELAS as for $t\bar{q}$ production. For the $t\bar{q}V$ signals there is an additional contribution from $t\bar{q}$ production plus radiative emission of a Z boson or a photon. This correction is suppressed because it does not have the enhancement due to the $\bar{t}$ on-shell, and is even smaller after the kinematical cuts for the signal reconstruction. We assume only one type of anomalous coupling different from zero at the same time, and give our results for the same chiralities used before. We check that for other chirality choices the differences are of order 0.1% for the three polarization options, before and after kinematical cuts. The backgrounds for the $t\bar{q}Z$ and $t\bar{q}\gamma$ signals are $W^+q\bar{q}'Z$ and $W^+q\bar{q}'\gamma$, with 46 and 44 diagrams, respectively. They are calculated with MadGraph.

After energy smearing and detector cuts, the $t\bar{q}\gamma$ signal can be reconstructed in a similar way as $t\bar{q}$. The W^+ momentum is the charged lepton momentum plus the missing momentum. The invariant mass of the W^+ and one of the jets, $m_t^{\rm rec}$, is consistent with the top mass, and the invariant mass of the photon and the other jet, $m_{\bar{t}}^{\rm rec}$, is also consistent with m_t. Of the two possible assignments, we choose the one minimizing $(m_t^{\rm rec} - m_t)^2 + (m_{\bar{t}}^{\rm rec} - m_t)^2$ and require a b tag on the jet that corresponds to the top quark. The reconstructed W^- mass $M_{W^-}^{\rm rec}$ is defined as the invariant mass of the two jets as before.

The reconstruction of the $t\bar{q}Z$ signal is slightly more complicated. Of the two positively charged leptons, one results from the W^+ decay and it has with the neutrino (reconstructed from the missing momentum) an invariant mass $M_{W^+}^{\rm rec}$ consistent with M_W. The other one and the negative charge lepton have an invariant mass $M_Z^{\rm rec}$ close to M_Z. If the two positive leptons have different flavours the assignment is straightforward, but if they have not we choose the pairing that minimizes $(M_{W^+}^{\rm rec} - M_W)^2 + (M_Z^{\rm rec} - M_Z)^2$. Then, we reconstruct the top and antitop masses as for the $t\bar{q}\gamma$ signal replacing the photon momentum by the Z momentum. The W^- reconstruction for the background is also similar.

In our analysis we find that all the signal cross-sections, including those with $\sigma_{\mu\nu}$ vertices, decrease raising the CM energy from 500 to 800 GeV, and for the latter the limits obtained are worse even after taking into account the increased luminosity. Hence we will discuss only the results for top decays at 500 GeV. We write the kinematical cuts in Table 7. The cut on $m_{\bar{t}}^{\rm rec}$ is more strict than the cut on $m_t^{\rm rec}$ because the reconstruction of the antitop mass is better. The cuts for $t\bar{q}Z$ are looser because the background is much smaller. Contrarily to $t\bar{q}$ production, the veto cuts on $M_{W^-}^{\rm rec}$ are not redundant. The cross-sections before and after cuts are collected in Table 8. Note that we normalize the signal to $X_{tq} = 0.2$, $\kappa_{tq} = 0.2$ $\lambda_{tq} = 0.04$ because the signal cross-sections are smaller.

Variable	$t\bar{q}Z$ cut	$t\bar{q}\gamma$ cut
$m_t^{\rm rec}$	$130 - 220$	$150 - 200$
$m_{\bar{t}}^{\rm rec}$	$150 - 200$	$160 - 190$
$M_{W^-}^{\rm rec}$	< 70 or > 90	< 65 or > 95

Table 7: Kinematical cuts for the $t\bar{q}V$ signals and the three polarization options at a CM energy of 500 GeV. The masses are in GeV.

	No pol.		Pol. e^-		Pol. e^- e^+	
	before cuts	after cuts	before cuts	after cuts	before cuts	after cuts
$t\bar{q}Z + \bar{t}qZ$ (γ_μ)	0.114	0.105	0.0784	0.0720	0.0995	0.0912
$t\bar{q}Z + \bar{t}qZ$ $(\sigma_{\mu\nu})$	0.0877	0.0809	0.0604	0.0555	0.0766	0.0703
$t\bar{q}\gamma + \bar{t}q\gamma$	0.0745	0.0631	0.0515	0.0429	0.0653	0.0543
$W^\pm jjZ$	0.0059	1.0×10^{-4}	0.0013	2.4×10^{-5}	8.9×10^{-4}	1.6×10^{-5}
$W^\pm jj\gamma$	0.639	0.0014	0.144	3.1×10^{-4}	0.0956	2.0×10^{-4}

Table 8: Cross-sections (in fb) before and after the kinematical cuts in Table 7 for the $t\bar{q}V$ signals and backgrounds at a CM energy of 500 GeV, for the three polarization options. We include b tagging efficiencies and use $X_{tq} = 0.2$, $\kappa_{tq} = 0.2$, $\lambda_{tq} = 0.04$.

For top decay signals the use of polarization is not as useful as for single top production. Although it reduces the W^+jjV cross-sections up to a factor of 7, these backgrounds are already very small for unpolarized beams, and the luminosities required to glimpse the potential improvement would exceed 1000 fb^{-1}. In addition, the signal cross-sections decrease $10 - 20\%$, in contrast to single top production, and the limits obtained are in some cases worse (see Table 9).

	No pol.		Pol. e^-		Pol. e^- e^+	
	95%	$3\,\sigma$	95%	$3\,\sigma$	95%	$3\,\sigma$
Br$(t \to Zq)$ (γ_μ)	1.8×10^{-3}	1.2×10^{-3}	2.7×10^{-3}	1.7×10^{-3}	2.1×10^{-3}	1.4×10^{-3}
Br$(t \to Zq)$ $(\sigma_{\mu\nu})$	1.9×10^{-3}	1.2×10^{-3}	2.8×10^{-3}	1.8×10^{-3}	2.2×10^{-3}	1.4×10^{-3}
Br$(t \to \gamma q)$	9.9×10^{-5}	1.3×10^{-4}	1.6×10^{-4}	1.6×10^{-4}	1.3×10^{-4}	8.3×10^{-5}

Table 9: Limits on top FCN decay branching ratios obtained from the $t\bar{q}V$ signals at 500 GeV with a luminosity of 300 fb^{-1} for the three polarization options.

The limits from the $t\bar{q}V$ signals are in all cases worse than those obtained from single top production, especially for Ztq couplings. In fact, these processes would only be useful if a FCN top decay is detected with Br$(t \to Zq) \sim 10^{-3}$ or Br$(t \to \gamma q) \sim 10^{-4}$. In such case, they would help to determine the nature of the top anomalous coupling. Besides, it is interesting to notice that the limits for Ztq γ_μ and $\sigma_{\mu\nu}$ couplings are remarkably similar, what confirms that top decays are not sensitive to the q^ν factor of the $\sigma_{\mu\nu}$ vertex.

4 Comparison with LHC

We have proved that, despite the relatively small single top and top pair production cross sections, TESLA is able to observe top FCN vertices corresponding to very small top decay branching ratios, or set competitive bounds on them if they are not observed. To obtain these results, beam polarization is essential to reduce the backgrounds. We now compare the best limits on anomalous couplings that can be obtained at TESLA and LHC. To obtain the values for LHC we rescale the data from the literature to a b tagging efficiency of 50% and keep the average mistagging rate used of 1% for other jets, which is somewhat optimistic. The best LHC limits on Vtc couplings come from top decays, whereas the best ones on Vtu

couplings are from single top production. The LHC limit on $\mathrm{Br}(t \to Zc)$ with $\sigma_{\mu\nu}$ couplings is estimated to be similar to the one with γ_μ couplings, since the same holds in our analysis for TESLA. We assume one year of running time in all the cases, that is, 100 fb^{-1} for LHC, 300 fb^{-1} for TESLA at 500 GeV and 500 fb^{-1} for TESLA at 800 GeV. We use the statistical estimators explained before.

	LHC		TESLA	
	95%	$3\,\sigma$	95%	$3\,\sigma$
$\mathrm{Br}(t \to Zu)$ (γ_μ)	6.2×10^{-5}	8.0×10^{-5}	1.9×10^{-4}	2.2×10^{-4}
$\mathrm{Br}(t \to Zc)$ (γ_μ)	7.1×10^{-5}	1.0×10^{-4}	1.9×10^{-4}	2.2×10^{-4}
$\mathrm{Br}(t \to Zu)$ $(\sigma_{\mu\nu})$	1.8×10^{-5}	2.3×10^{-5}	6.2×10^{-6}	7.0×10^{-6}
$\mathrm{Br}(t \to Zc)$ $(\sigma_{\mu\nu})$	7.1×10^{-5}	1.0×10^{-4}	6.2×10^{-6}	7.0×10^{-6}
$\mathrm{Br}(t \to \gamma u)$	2.3×10^{-6}	3.0×10^{-6}	3.7×10^{-6}	3.6×10^{-6}
$\mathrm{Br}(t \to \gamma c)$	7.7×10^{-6}	1.2×10^{-5}	3.7×10^{-6}	3.6×10^{-6}

Table 10: Best limits on top FCN couplings that can be obtained at LHC and TESLA after one year of operation.

We see that LHC and TESLA complement each other in the search for top FCN vertices. The γ_μ couplings to the Z boson can be best measured or bound at LHC, whereas the sensitivity to the $\sigma_{\mu\nu}$ ones is better at TESLA. For photon vertices, LHC is better for γtu and TESLA for γtc. The complementarity of LHC and TESLA also stems from the fact that TESLA will not be able to distinguish Ztq and γtq couplings in the limit of its sensitivity, whereas LHC will because final states are different and distinguish between them. On the other hand, the good charm tagging efficiency expected at TESLA will allow to distinguish Vtu and Vtc couplings looking at the flavour of the final state jet, what is more difficult to do at LHC.

Acknowledgements

I am indebted to T. Riemann for many useful discussions. I also thank F. del Aguila and A. Werthenbach for a critical reading of the manuscript and S. Slabospitsky for useful comments. I thank the members of the Theory group of DESY Zeuthen for their warm hospitality during the realization of this work. This work has been supported by a DAAD scholarship and by the European Union under contract HTRN–CT–2000–00149

References

[1] For a review see M. Beneke, I. Efthymipopulos, M. L. Mangano, J. Womersley (conveners) *et al.*, report in the *Workshop on Standard Model Physics (and more) at the LHC*, Geneva, hep-ph/0003033

[2] G. Eilam, J. L. Hewett and A. Soni, Phys. Rev. **D44**, 1473 (1991)

[3] F. del Aguila, J. A. Aguilar-Saavedra and R. Miquel, Phys. Rev. Lett. **82**, 1628 (1999)

[4] D. Atwood, L. Reina and A. Soni, Phys. Rev. **D55**, 3156 (1997)

[5] J. M. Yang, B. Young and X. Zhang, Phys. Rev. **D58**, 055001 (1998)

[6] F. del Aguila and M. J. Bowick, Nucl. Phys. **B224**, 107 (1983); K. Higuchi and K. Yamamoto, Phys. Rev. **D 62**, 073005 (2000)

[7] J. Yang and C. Li, Phys. Rev. **D 49**, 3412 (1994); J. Guasch and J. Sola, Nucl. Phys. **B562**, 3 (1999); S. Bejar, J. Guasch and J. Sola, hep-ph/0011091

[8] V. Obratzsov, talk given at ICHEP 2000, Osaka, July 2000

[9] ALEPH Collaboration, CERN-EP-2000-102, Phys. Lett. **B** (in press); see also the contributed papers of the DELPHI Collaboration, L3 Collaboration and OPAL Collaboration to ICHEP 2000

[10] F. Abe *et al.* [CDF Collaboration], Phys. Rev. Lett. **80**, 2525 (1998)

[11] T. Stelzer, Z. Sullivan and S. Willenbrock, Phys. Rev. **D58**, 094021 (1998)

[12] T. M. Tait and C. P. Yuan, hep-ph/9710372; T. M. Tait, Phys. Rev. **D61**, 034001 (2000)

[13] T. Han, R. D. Peccei and X. Zhang, Nucl. Phys. **B454**, 527 (1995)

[14] T. Han, K. Whisnant, B.-L. Young and X. Zhang, Phys. Rev. **D55**, 7241 (1997)

[15] T. Han, K. Whisnant, B.-L. Young and X. Zhang, Phys. Lett. **B385**, 311 (1996)

[16] J. A. Aguilar-Saavedra and G. C. Branco, Phys. Lett. **B495**, 347 (2000)

[17] F. del Aguila, J. A. Aguilar-Saavedra and Ll. Ametller, Phys. Lett. **B462**, 310 (1999); F. del Aguila and J. A. Aguilar-Saavedra, Nucl. Phys. **B576**, 56 (2000)

[18] M. Hosch, K. Whisnant and B.-L. Young, Phys. Rev. **D56**, 5725 (1997)

[19] V. F. Obraztsov, S. R. Slabospitsky and O. P. Yushchenko, Phys. Lett. **B426**, 393 (1998); T. Han and J. L. Hewett, Phys. Rev. **D60**, 074015 (1999); S. Bar-Shalom and J. Wudka, Phys. Rev. **D60**, 094016 (1999)

[20] E. Murayama, I. Watanabe and K. Hagiwara, KEK report 91-11, January 1992

[21] T. Stelzer and W. F. Long , Comput. Phys. Commun. **81**, 357 (1994)

[22] S. Bertolucci, talk given at the *'5th Workshop of the 2nd ECFA/DESY Study on Physics and Detectors for a Linear Electron - Positron Collider'*, Obernai 16-19 October, 1999

[23] C. Damerell, talk given at the *'7th Workshop of the 2nd ECFA/DESY Study of Physics and Detectors for a Linear Electron-Positron Collider'*, DESY Hamburg, 22-25 September, 2000

[24] G. J. Feldman and R. D. Cousins, Phys. Rev. **D57**, 3873 (1998)

[25] J. A. Aguilar-Saavedra, Comput. Phys. Commun. **130**, 190 (2000)

[26] G. Cowan, Statistical Data Analysis, Oxford University Press, 1998